Title:

Enhanced TCR footprint by a novel glycolipid increases NKT-dependent tumor protection

Author(s): Sandrine Aspeslagh, Marek Nemčovič, Nora Pauwels, Koen Venken, Jing Wang, Serge Van Calenbergh, Dirk M. Zajonc and Dirk Elewaut

Source: JOURNAL OF IMMUNOLOGY (2013), 191 (6) ,2916-2925 **DOI:** 10.4049/jimmunol.1203134

Enhanced TCR footprint by a novel glycolipid increases NKT dependent tumor protection.

Running Title: Effects of a novel glycolipid with enhanced NKTCR footprint

Sandrine Aspeslagh*§, Marek Nemčovič†§, Nora Pauwels‡, Koen Venken*, Jing Wang†, Serge Van Calenbergh‡, Dirk M. Zajonc†¶ and Dirk Elewaut*¶

*Laboratory for Molecular Immunology and Inflammation, Department of Rheumatology, Faculty of Medicine and Health Sciences, Ghent University, Ghent, Belgium.

†Division of Cell Biology, La Jolla Institute for Allergy and Immunology, La Jolla, CA 92037, USA

‡Laboratory for Medicinal Chemistry, Faculty of Pharmaceutical Sciences, Ghent University, Ghent, Belgium

§These authors contributed equally

¶These authors shared supervision of the work

¶To whom correspondence should be addressed:

Dirk Elewaut, MD, PhD, Laboratory for Molecular Immunology and Inflammation, Department of Rheumatology, Ghent University, De Pintelaan 185, 9000 Ghent, Belgium. Phone +32(9)3322240, Fax. +32(9)3323803. Email: Dirk.elewaut@ugent.be

Dirk M. Zajonc, PhD, Division of Cell Biology, La Jolla Institute for Allergy and Immunology, 9420 Athena Cir, La Jolla, CA 92037, USA. Phone +1(858)7526605, Fax. +1(858)7526985. Email: dzajonc@liai.org

Abstract

NKT cells, a unique type of regulatory T cells, respond to structurally diverse glycolipids presented by CD1d. While it was previously thought that recognition of glycolipids such as α-GalCer by NKTCR obeys a key-lock principle, it is now clear this interaction is much more flexible. Here, we report the structure-function analysis of a series of novel 6”-OH analogues of α-GalCer with more potent anti-tumor characteristics. Surprisingly, one the novel carbamate analogues, PyrC- α-GalCer, formed novel interactions with the NKTCR. This was associated with an extremely high level of Th1 polarization and superior anti-tumor responses. These data highlight the *in vivo* relevance of adding aromatic moieties to the 6”-OH position of the sugar and additionally show that judiciously chosen linkers are a promising strategy to generate strong Th1 polarizing glycolipids through increased binding either to CD1d or NKTCR.

Introduction

NKT cells are a subset of regulatory T cells that are involved in different pathological processes, ranging from autoimmunity to protection against tumors and bacterial infections (1). NKT cell activation results in cytotoxicity, proliferation and also rapid cytokine production (within several hours), which subsequently activate several bystander immune cells (NK cells, dendritic cells, B cells, etc). They have the capacity to produce both Th1 and Th2 cytokines and to modulate production by bystander cells. As such they have the ability to lead to Th biased responses under certain conditions. Although recently a lot of studies have been performed to unravel the mechanism for Th1/Th2 polarization (2-7), much remains to be uncovered.

These innate-like T cells recognize glycolipids in the context of CD1d, which is a monomorphic MHC I like molecule that accommodates the lipid tails of the glycolipid in two hydrophobic pockets (A' and F') and presents the sugar head to the NKTCR. The prototype iNKT-cell activating glycolipid is alpha-galactosylceramide (α-GalCer) whose chemical structure consists of a 26 carbon acyl chain and a phytosphingosine chain alpha anomerically linked to galactose. Although initially iNKT cell research was mainly focused on this antigen, the list of novel glycolipids that are able to induce iNKT cell activation is continuously growing and includes very diverse bacterial antigens and endogenously expressed glycolipids, in addition to newly synthesized antigens (8, 9).

The iNKT cell TCR is semi-invariant as it contains a conserved V□14 chain in mice and V□24 in human that both re-arrange with J□18, while the Vβ chain is more variable. However, only germline encoded residues are important for the recognition of a glycolipid (10). Although the TCR plays an important role for initial recognition of the CD1d-glycolipid complex, the strength of a Th1 polarized iNKT cell dependent activation seems to be more determined by the stability of the CD1d-glycolipid complex. Previously we showed that NU- α-GalCer induces a structural change within the A' roof of CD1d to which it binds with its hydrophobic 6"-naphthylurea group, leading to the so called third anchor model (7). However extra binding strength of a glycolipid can also be achieved through alterations of the lipid tails (11, 12). The altered sphingosine chain of a plakoside analog was shown to increase the contact surface area with CD1d within the F'-pocket (6). Additionally it was shown that several acyl chain altered glycolipids can induce superior anti-cancer effects compared to α-GalCer and this was also linked to increased CD1d avidity (13). OCH on the other hand, has a shorter sphingosine chain (C9 instead of C18) and is therefore not able to induce the formation of the F' roof in CD1d which affects the recognition by the NKTCR and thus its antigenicity (5, 14). Last but not least crystallographic analysis of bacterial glycosyl-diacylglycerol lipids, as well as iGb3, which is a beta-anomeric tri-hexose containing sphingolipid self-antigen demonstrated that the TCR was able to "bulldoze" the three sugar groups over the CD1d-surface,

thus allowing the TCR to bind to the CD1d-glycolipid complex with its conserved footprint (15-18). For iGb3, this mechanism induces the last "anchor" sugar to bind to CD1d, however this doesn't appear to happen to Gb3, which only differs by an altered linkage of the last sugar, because the position of the terminal sugar of Gb3 likely does not favor the formation of this additional anchor to CD1d (17). However, a similar, yet energetically unfavorable linker can be enforced in Gb3 through mutation of the TCR to reach sufficiently high auto-reactivity for CD1d (18). Besides its role in enhancing Th1 polarization, the stability of the CD1d-glycolipid complex also seems to determine the antigenicity of certain glycolipids for iNKT cells. It was demonstrated for α-C-GalCer, a well-known Th1 polarizing glycolipid with anti-tumor properties, that its complex with CD1d had a much longer half-life *in vivo* than the corresponding CD1d- α-GalCer complexes (5). Therefore structural features that enhance the binding stability between a glycolipid and CD1d seem to enhance both its antigenicity and its Th1 polarizing properties.

Our previous data suggested that the formation of an extra anchor between a glycolipid and CD1d confers to stronger anti-tumoral responses *in vivo*. However, the Th1 polarizing strength seemed to be critically dependent on the nature and length of the linker between C-6" of the galactose and the aromatic group. BnNH-GSL-1', an analogue that is characterized by an aromatic moiety that is located one atom closer to the galactose ring, was shown to exhibit weaker TCR affinity and decreased antigenicity. Despite the fact that this glycolipid also carries an amide linker, similar to the urea linker of NU- α-GalCer, it does not form an additional anchor with CD1d, likely as a result of the different linker length (7). To explore the structural modifications that are required for the formation of the third anchor, three novel 6"-OH altered glycolipids were synthesized containing a carbamate linker, which has the same length as NU- α-GalCer but increased flexibility. They are able to induce superior Th1 responses in mice and also activate human iNKT cells. In contrast to most Th1 polarizing analogs the Th1 polarization potency did not only depend on the induction of a different Th1/Th2 polarization balance but also on a much higher induction of Th1 cytokines compared to α-GalCer, which was independent of the mode of administration. We show that in analogy to NU- α-GalCer these carbamates display an increased binding stability for CD1d compared to α-GalCer, further emphasizing the relevance of this model in iNKT cell driven responses. Additionally we demonstrate that one glycolipid exhibits better anti-tumor activity than NU- α-GalCer. Surprisingly, structural characterization of two of the potent carbamate glycolipids revealed that none of the aromatic groups form the third anchor to the degree observed for NU- α-GalCer. Instead, the most potent Th-1 skewing glycolipid PyrC- α-GalCer does form an additional "anchor" with the TCR, leading to highest observed TCR binding affinity of all studied α-GalCer analogs to date but equal to that of α-GalCer itself.

Material and Methods

Synthetic glycolipids

Glycolipids were synthesized in the lab of Medicinal Chemistry (19). α-C-GalCer was kindly provided M.Tsuji (Aaron Diamond AIDS Research Center, NY, USA) and the NIH Tetramer Core Facility. Lyophilized glycolipids were dissolved in pure DMSO (Sigma) at 10 mg/mL concentration and stored at -20˚C. Glycolipids were further solubilized by adding PBS (Invitrogen) or vehicle (96 mg/mL sucrose, 10 mg/mL sodium deoxycholate, 0,05 % Tween 20), warming to 80°C for 20 minutes, sonication for 10 minutes.

Cell Lines

The murine iNKT hybridoma N38-2C12 (Vα14Vβ8.2*b*) was provided by L. Brossay (20) (Brown University, Providence, RI, USA). Cells were cultured in DMEM (Sigma) supplemented with 10% fetal calf serum (Invitrogen), 1% glutamine (Sigma), 1% penicillin streptomycin (Sigma), and 2-mercaptoethanol (Sigma) (called cDMEM hereafter). B16 melanoma cells were cultured in advanced RPMI (Sigma) supplemented with 10% fetal calf serum (Invitrogen), 1% glutamine (Sigma) and 1% penicillin streptomycin (Sigma). They were harvested using cell dissociation buffer, which was washed away twice first using the medium and second with PBS. 400 000 cells were IV injected within 30 minutes after harvest into the tail vein.

Isolation and expansion of BMDCs.

BMDCs were isolated from the mouse bone marrow as described previously (21).

Mice

C57BL/6 and CD45.1 mice were in house bred (in accordance with the general recommendations for animal breeding and housing) or purchased from the Harlan Laboratory, Jα18-knockout mice on the C57BL/6 background were kindly provided by M. Taniguchi (22) (RIKEN, Tsurumi, Yokohama, Japan). Experiments were conducted according to the guidelines of the Ethical Committee of Laboratory Animals Welfare of Ghent University. Mice used for experiments were between 5 and 12 weeks old.

In vivo tumor model

Within 30 minutes after harvesting, a dose of $2x10^5$ or $4x10^5$ cells B16 cells were inoculated intravenously (tail vein). Mice were killed 14 days later, the lungs were removed, and surface

metastases were counted with the aid of a dissecting microscope.

In Vitro and In Vivo Activation of iNKT Cells

For *in vitro* stimulation, murine iNKT hybridoma cells at $5x10^4$ cells/well in 96-well plates were stimulated with the 10^5 cells/well glycolipid pulsed BMDCs in cDMEM for 4, 16 or 24 hours at 37˚C, and levels of murine IL-2 secretion were determined by ELISA.
For *in vivo* activation of iNKT cells C57BL/6 mice were either intraperitoneally injected with 5 µg glycolipid (dissolved in PBS) or intravenously with $6x10^4$ or $1x10^4$ glycolipid pulsed BMDCs.

Isolation of human PBMCs and iNKT cells

Human iNKT cells from healthy adult individuals were sorted and expanded as described previously (7). PBMCs were isolated by means of density centrifugation, incubated overnight in the presence of indicated glycolipids (100 ng/ml), washed and irradiated (40 Gy). Subsequently, $5x10^4$ iNKT cells were stimulated with 10^5 glycolipid pulsed autologous PBMCs in RPMI 1640 media supplemented with 10% human AB serum (Lonza), 1% sodium pyruvate, 1% nonessential amino acids and 1% penicillin/streptomycin (all from Invitrogen). Supernatants were collected after 24hrs of culture and cytokine levels were determined by means of cytometric Bead Arrays (CBA) following the manufacturer's instructions (BD).

Isolation of murine lymphocytes

Spleen cells were isolated as previously described (23). Lymphocytes were isolated at the interface and washed, depleted with an anti-CD3 kit (Miltenyi) and resuspended in staining buffer containing saturating amount of anti-Fcγ Receptor type II/type III monoclonal antibodies (Miltenyi Biotec, Sunnyvale, CA). Hereafter cells were stained with fluorochrome-conjugated mAbs (all from eBioscience) directed against the described antigens. Live cells (exclusion with DAPI) were acquired on a FACSCanto (BD) flow cytometer and analyzed using FlowJo (Tree Star) software.

Surface Plasmon Resonance experiments

Glycolipids were dissolved in DMSO at 1 mg/ml and stored at -20^{o}C. SPR studies were conducted using a Biacore 3000 as reported previously (24). Briefly, biotinylated birA-tagged mCD1d protein was loaded o/n with 6-times molar excess of glycolipids as previously reported (16) and 500 – 600 RU of mCD1d-glycolipids complexes were captured on a streptavidin sensor chip surface (GE Healthcare). TCR protein was diluted in detergent-free running buffer (10 mM Hepes, 150 mM NaCl, and 3 mM EDTA, pH 7.4). The TCR was injected in serial dilutions (0, 0.0156 – 2 µM) for 1.5 – 3 min at 30 µl/min to measure the association phase, while dissociation was continued for 45

min at 25°C. A reference surface containing "empty" CD1d was generated in flow channel one of the streptavidin sensor chip and its TCR binding response was subtracted from the other sensorgrams before calculating binding kinetics using a simple Langmuir 1:1 model in the BIA evaluation software version 4.1. Experiments were performed three times, each using a different TCR preparation.

Crystallization and Structure Determination

The ternary mCD1d-lipid-mTCR complexes using the lipids 4ClPhC-α-GalCer and PyrC-α-GalCer were prepared as described previously for NU-α-GalCer (7) and purified by size exclusion chromatography (SEC) using Superdex S200 10/300 GL (GE Healthcare). Both mCD1d-4ClPhC-α-GalCer-mTCR and mCD1d-PyrC-α-GalCer-mTCR complexes were concentrated to 3.5 mg/ml in SEC buffer (50 mM Hepes, pH 7.5, 150 mM NaCl). Crystals were grown at 22.3°C by sitting drop vapor diffusion while by mixing 0.5 µl mCD1d-4ClPhC-α-GalCer-mTCR and 0.5 µl precipitate (20% PEG 4000, 0.2 M sodium thiocyanate) or by mixing 1 µl mCD1d-PyrC-α-GalCer-mTCR and 1 µl precipitate (20% PEG 4000, 0.2 M di-ammonium hydrogen citrate), respectively.

Crystals were flash-cooled at 100 K in mother liquor containing 30% glycerol. Diffraction data from a single crystal were collected at the Stanford Synchrotron Radiation Laboratory beamlines 9-2 (mCD1d-4ClPhC-α-GalCer-mTCR) and 11-1 (mCD1d-PyrC-α-GalCer-mTCR), and were processed with the HKL2000 (25) and iMosflm (26) software to 3.0 Å, and 2.8 Å resolution, respectively. The mCD1d-4ClPhC-α-GalCer-mTCR crystal belongs to orthorhombic space group $C222_1$ with cell parameters a = 79.28 Å, b = 191.86 Å, and c = 151.59 Å. The mCD1d-PyrC-α-GalCer-mTCR crystal also belongs to space group $C222_1$ with cell parameters a= 78.97 Å, b= 191.40 Å, and c= 151.22 Å.

The asymmetric unit contains one mCD1d-glycolipid-TCR molecule with estimated solvent content of 57.3 % based on a Matthews' coefficient (Vm) of 2.88 A^3/Da for 4ClPhC-α-GalCer and 56.9 % (VM) of 2.86 A^3/Da for PyrC-α-GalCer. Crystal structures were determined by molecular replacement using MOLREP (27) as part of the CCP4 suite (28). Protein coordinates from mCD1d-iGB3-mTCR (from Protein Data Bank code 3RZC), as the search model, with the ligand removed, were used for molecular replacement (MR) for mCD1d-PyrC-α-GalCer-mTCR. The protein mCD1d coordinates from the mCD1d-iGB3 structure (from PDB 2Q7Y) and the mouse Vα14Vβ8.2 TCR (from PDB 3QUY) coordinates were used for mCD1d-4ClPhC-α-GalCer-mTCR structure determination by MR. The REFMAC glycolipid libraries, were created using the Dundee ProDRG2 server (29). After the MR solutions for both crystal structures were obtained, containing both mCD1d and mTCR, the model was rebuilt into σ_A –weighted $2F_o$-F_c and F_o-F_c difference electron

density maps using the program COOT (30). Final refinement steps were performed using the translation, libration and screw axis (TLS) procedure in REFMAC(31) with five anisotropic domains (α1-α2 domain of mCD1d, including carbohydrates and glycolipids, α3-domain, β2m, variable domain, and constant domain of mTCR). The mCD1d-PyrC-α-GalCer-mTCR structure has the final R_{cryst} = 19.13% and R_{free} = 23.94% and was refined to 2.8 Å, while mCD1d-4ClPhC-α-GalCer-mTCR was refined to 3.00 Å with a final R_{cryst}= 18.59% and R_{free}= 22.84%. The high quality of both models was confirmed with the program Molprobity (32).

Statistical analysis

The statistical test used throughout this study was Kruskal-Wallis test with Dunn's multiple comparison test or Mann Whitney U test (unpaired, two-sided) unless otherwise stated. Data was analyzed using Excel (Microsoft) and Graphpad Prism 5.

Results

Previously we have shown that α-GalCer analogs with alterations at the 6" position of the sugar head group are potent inducers of iNKT cell dependent IFN-γ production. It was suggested that this would depend on the length of the linker between the sugar and the aromatic moiety. Crystallographic analysis of the tri-molecular complex with NU-α-GalCer showed that the latter makes an additional anchor to CD1d thereby stabilizing the interaction with CD1d (7). In NU-α-GalCer this linker is urea-based. However, if the chemical nature of the linker is critically important in determining the strong iNKT cell response was still unclear. From a synthesis point of view, a 6"-*O*-based instead of a 6"-*N*-based derivatisation, could significantly improve the accessibility of 6"-derivatives, since the route towards the former modification is typically 3 steps shorter. To explore this enigma, three novel glycolipids were synthesized containing a carbamate-based linker instead of the urea (Figure 1) using a recently reported synthesis, which allows to selectively derivatise the 6"-OH, after regioselective opening of a 4",6"-*O*-benzylidene ring (33).

Carbamates are strong Th1 polarizers *in vivo*

To assess the antigenicity of these carbamate analogues and their ability to induce Th1-skewing, mice were bled at 16 hours after i.p. glycolipid exposure because this is known to afford peak levels of IFN-γ, the hallmark Th1 cytokine. Strikingly, all carbamate-linked glycolipids induced significantly higher IFN-γ levels than NU-α-GalCer and α-GalCer (Figure 1). In this setting, NU-α-GalCer induced comparable or slightly lower IFN-γ production compared to α-GalCer. IFN-γ production in response to glycolipid dependent iNKT cell activation is known to be dependent on IL-12 (34-36), which was therefore analyzed. As expected also IL-12 production was significantly higher for the carbamate-based glycolipids compared to α-GalCer. However, only PyrC-α-GalCer was capable of inducing significantly higher IL-12 levels than NU-α-GalCer. Administration of these novel glycolipids to Jα18-/- mice, which lack iNKT cells, did not induce any cytokine production, thereby excluding non-specific effects (Supplementary Figure 1).

Next we examined if the glycolipid pulsed BMDCs behave similarly *in vivo*. For cytokine analysis we bled the mice at several time points after injection. We focused on IFN-γ and IL-12 secretion. Again at 16 hours both carbamates induced a significantly higher IFN-γ secretion compared to NU-α-GalCer (which in this context is also significantly higher than α-GalCer) (Figure 2). Strikingly for PyrC-α-GalCer the IFN-γ level increased up to 24 hours after injection in contrast to 4ClPhC-α-GalCer and NU-α-GalCer. Similarly IL-12 secretion was very high with PyrC-α-GalCer and even after 24 hours markedly higher than for NU-α-GalCer. Furthermore, PyrC-α-GalCer and the other 6"-OH altered glycolipids were also able to induce Th1-biased cytokine secretion (more IFN-γ and

IL-12 and less IL-4 and IL-13 compared to α-GalCer) in cultures of purified human iNKT cells (Figure 3 and data not shown). A similar trend was seen with human peripheral blood mononuclear cells (PBMCs) (data not shown) highlighting the conserved nature of the Th polarization.

6"-OH analogs modulate the co-stimulatory landscape

Expression of co-stimulatory markers at the cell surface is linked to cytokine polarization because this determines the degree of activation of bystander cells such as NK cells, whose IFN-γ production is responsible for Th1 polarized cytokine profile (37). For α-C-GalCer, it has been shown that expression of CD40 is essential for IL-12 and subsequent NK cell dependent IFN-γ production (3). Additionally OX40L upregulation by DCs has been found important for α-GalCer dependent tumor killing (38). Here we show that PyrC-α-GalCer, which induces the highest levels of IL-12, induces early CD40 and OX40L upregulation on spleen DCs (CD11c CD11b double positive) both quantitatively and qualitatively (Supplementary Figure 2). ICOSL expression has been related to production of Th2 cytokines by MZB cells (39) and was shown to be important for cytokine production and survival of CD4 positive iNKT cells (40). The shifts in ICOSL expression were overall minimal, so the exact relationship between ICOSL expression and the superior Th1 polarization by PyrC-α-GalCer remains to be determined. Glycolipid stimulation of iNKT cells leads to CD28 expression, and induces CD80 and CD86 expression at the dendritic cell surface, which is required for induction of IL-12 by dendritic cells (41). This was confirmed here as all glycolipids including α-GalCer induced upregulation of both CD80 and CD86.

TCR affinity and stability of the CD1d- glycolipid complex

iNKT cell polarization is a matter of debate and it has been shown that uptake by different cells can also affect the outcome (42, 43). To avoid these host dependent parameters we set up a simple *in vitro* model, which consists of co-cultures of glycolipid pulsed bone marrow dendritic cells and an iNKT cell hybridoma (i.c. 2C12 containing a Vβ8.2 TCR (44)). IL-2 production is used as a read-out for TCR affinity for the whole CD1d-glycolipid complex. Here the carbamates, NU-α-GalCer and α-C-GalCer induce higher IL-2 levels (Figure 4). To confirm this we also measured intracellular IL-2 production in 2C12 cells already 4 hours after co-culture, where a similar result was obtained (Figure 4). It was reported that bone marrow dendritic cells (BMDCs) can also produce IL-2 (45), however intracellular IL-2 staining of BMDCs was negative (data not shown). Because IL-2 production is a downstream event of TCR signaling we analyzed TCRβ expression. *In vivo* it is well known that iNKT cells internalize their TCR upon antigen recognition (46). Figure

4 suggests that TCR internalization also occurs *in vitro* and correlates well with the intracellular IL-2 production.

However, IL-2 production and TCR triggering are the result of both molecular TCR affinity and CD1d stability. Therefore, we assessed the equilibrium binding constants (K_D) of the TCR towards the different glycolipids presented by CD1d, using surface plasmon resonance. Overall the data show similar affinities for the tested glycolipids PyrC-α-GalCer (K_D=25 nM), α-GalCer (K_D=26 nM), NC-α-GalCer (K_D=37 nM) and 4ClPhC-α-GalCer (K_D=49.3 nM) (Table I). Thus in contrast to BnNH-GSL-1' the glycolipid presentation by CD1d and/or the glycolipid interaction with the TCR is not significantly affected by the carbamate linked aromatic groups. While 4ClPhC-□-GalCer shows a 2-fold reduced binding affinity (49 nM vs. 25 nM), the structurally related PyrC-□-GalCer has a binding affinity equal to that of □GalCer (25 nM). Therefore, the slightly different 6"-OH modifications also translate into only marginally different binding affinities of the TCR, suggesting similar binding chemistries with the TCR. Secondly, we investigated the role of CD1d-glycolipid stability, which has recently been shown to be important for antigenic iNKT responses (6, 7, 13). We used a cellular assay to determine the binding stability of the novel glycolipids. Bone marrow dendritic cells were loaded with 100 ng/mL glycolipid during 20 hours. After removal of the free glycolipid, cells were left in appropriate medium for several time intervals (ranging from 4h to 48h). Dissociated glycolipid was removed and co-culture with 2C12 cells was initiated. IL-2 production in the medium was used as a surrogate marker for remaining CD1d with glycolipid. The strong Th1 polarizing α-C-GalCer, characterized by a higher binding stability to CD1d, was also included into this assay. IL-2 levels were normalized to the values of 4 hours after wash off to exclude the effect of TCR affinity. Figure 5B clearly shows that all 6"-OH analogs and α-C-GalCer behave very similarly and have a much slower decay compared to α-GalCer. We conclude that all tested Th1 analogs have a similar stability with CD1d *in vitro*, which is much higher than for the CD1d-α-GalCer complex.

Crystal structure of the mCD1d-PyrC-α-GalCer-TCR and mCD1d-4ClPhC-α-GalCer-TCR ternary complexes

We previously reported the structural details of how another potent Th1 skewing glycolipid, NU-α-GalCer interacts with CD1d and the TCR of iNKT cells (7). In that case the NU-group faces down into the CD1d binding groove to form an additional anchor with CD1d, leading to increased CD1d stability. We, therefore sought to determine whether the glycolipids PyrC-α-GalCer and 4ClPhC-α-GalCer follow a similar binding mode, since their 6" modifications are connected to the galactose of α-GalCer via a more flexible carbamate linker (Figure 1). We determined the crystal structures of the ternary complexes CD1d-PyrC-α-GalCer-TCR and CD1d-4ClPhC-α-GalCer-TCR to resolutions

of 2.8 Å and 3 Å, respectively (Supplementary table 1 and Figure 6)[ii]. Surprisingly, while the binding of both glycolipids is highly similar to that of α-GalCer, neither of the aromatic substitutions of PyrC-α-GalCer and 4ClPhC-α-GalCer insert down into the CD1d binding groove, as has been demonstrated for NU-α-GalCer (Figure 6). Instead, both 6”-OH aromatic substitutions are presented differently above the A’ pocket of CD1d. While 4ClPhC-α-GalCer does not induce a structural change in the A’ roof of CD1d, it interacts more intimately with CD1d. In contrast, PyrC-α-GalCer is slightly elevated and its pyridine group contacts the TCR (Figure 6B, C). Similar to α-GalCer, the galactose moiety of both glycolipids forms H-bonds with the TCR through the 2’’-and 3’’-OH groups, while the 4’’-OH group looses this contact. Interestingly, it has been shown that the TCR contact with the 4”-OH group is the key determinant in TCR interaction (14). However, both PyrC-α-GalCer and 4ClPhC-α-GalCer lost the H-bond (while still making a VdW contact with 3.5 – 3.8 Å distance) and still have similar binding affinities compared to α-GalCer, suggesting that the 6”-OH modifications compensate in part for the loss of the 4”-OH H-bond with the TCR. Most surprisingly, major van der Waals (VdW) interactions were observed between the pyridine of PyrC-α-GalCer and the Gln52 of the TCR (Figure 6C). The pyridine makes intimate contacts with Gln52 (distance 3.3 – 3.5 Å) compared to 6.4 – 6.9 Å for the 4Cl-phenyl group (4ClPhC-α-GalCer) and 8.0 – 12.9 Å for the napthtyl group (NU-α-GalCer) (Figure 7). As a result, the TCR exhibits many more interaction with PyrC-α-GalCer than with 4ClPhC-α-GalCer or NU-α-GalCer (7) leading to the observed high affinity TCR binding (Table 1). Even though the pyridine ring forms extra contacts with Gln52 of the TCR, the binding affinity does not exceed the binding affinity of mTCR to α-GalCer-CD1d, likely as it lacks the important H-bond with between the 4”-OH of galactose and Asn30 of the TCR. Interestingly, the additional glycolipid contact with TCR residue Gln52 has previously not been seen in any other structure. Therefore, our data provide a structural framework for the design of novel α-GalCer analogs that target Gln52 to increase TCR contacts.

Binding of 4ClPhC-α-GalCer and PyrC-α-GalCer to CD1d equals that of α-GalCer. All the H-bond interactions between the 2’’-OH (with Asp153) and 3’’-OH (with Asp153) of the glycolipid galactose and the 3-OH (with Asp80), 4-OH (with Asp 80) of the glycolipid ceramide backbone with CD1d residues (outlined) are conserved (Figure 6D). Carbamate linked aromatic groups of 4ClPhC-α-GalCer and PyrC-α-GalCer, however, do not form the extra H-bond interactions between the carbonyl oxygen of the urea linker that connects the galactose and the naphthyl moieties with Thr159 of CD1d as shown in urea linked NU-α-GalCer. Thus the carbamate linker results in a more flexible presentation of the substituents as well as a less tight interaction of the linker itself with CD1d, explaining the slightly less well ordered electron density for the glycolipid 6”-OH modification, versus NU-α-GalCer (Figure 6B) (7). Analysis of the buried surface areas (a measure of the extend of how two molecules contact each other) between the glycolipids and CD1d indicates

that 4ClPhC-α-GalCer binds as extensively to CD1d as NU-α-GalCer (1,124 vs. 1146 Å^2), correlating with their enhanced CD1d-stability (Figure 5B), while PyrC-α-GalCer (1,045Å^2) and α-GalCer (1,027 Å^2) interact less extensively with CD1d (Table 2). PyrC-α-GalCer, however, interacts more with the TCR α–chain (199.2 Å^2 vs. 137.1-155.7 Å^2) and also shows an increased stability when bound to CD1d (Figure 5B). The increased contacts of 4ClPhC-α-GalCer are mostly the result of novel or increased vdW interactions with CD1d residues including Met69, Met162 and more importantly, Thr159 (Supplemental Table S2). Glycolipid contacts with Thr159 are not formed when α-GalCer or PyrC-α-GalCer bind to CD1d.

As a result, we observe two different glycolipid binding modes compared to α-GalCer. Glycolipids that form increased contacts with CD1d (NU-α-GalCer and 4ClPhC-α-GalCer) and glycolipids that form increased contacts with the TCR (PyrC-α-GalCer). In addition, our data suggests that the tested 6"-OH modified α-GalCer analogs have generally increased stability when loaded on CD1d, even in the absence of obvious additional molecular contacts with CD1d. In addition, our data show that the stability of the CD1d-carbamate glycolipid complexes is highly similar to that of NU-α-GalCer and much higher than that of α-GalCer (Figure 5), suggesting a currently not well understood role of the aromatic 6"-OH modification for the overall CD1d-glycolipid stability.

Comparison of the presentation of both carbamate-linked, as well as urea-linked aromatic substitutions reveals the paucity of binding orientations that are adopted by the different chemical groups (Figure 7). From forming a third anchor inside CD1d (NU-α-GalCer) to forming intimate contacts with the TCR (PyrC-α-GalCer), the aromatic groups bridge about 11 Å between the CD1d and TCR interface with the capacity to induce structural changes within CD1d, depending on the composition of the linker and aromatic substitution.

Carbamate-pulsed BMDCs confer to strong anti-metastatic potential

In order to determine if the new glycolipids can also mimic the anti-metastatic activity of NU-α-GalCer, we examined their impact in the B16 lung melanoma model. Even though NU-α-GalCer was significantly stronger compared to α-GalCer, PyrC-α-GalCer was still superior in preventing tumor metastasis in the B16 lung model (Figure 8). As little as 10^4 pulsed BMDCs were enough to exert this marked tumor response. To analyze if this anti-tumor efficacy corresponds to strong cytokine responses mice were bled 16 hours after injection of 10 000 pulsed bone marrow dendritic cells. Similar to the cytokine results with the high dose and the anti-metastatic results, PyrC-α-GalCer caused significantly higher IL-12 and IFN-γ production (Figure 2 c+d).

Discussion

We report the results of a novel group of 6”-OH analogs with superior Th1 polarizing potential. Previously described Th1 polarizing glycolipids mostly exhibited weaker antigenicity and their Th1 polarization mainly stemmed from a much weaker Th2 cytokine production (3, 13, 47). In contrast, the carbamate-analogs described here display a significantly stronger Th1 profile due to significantly higher IFN-γ and IL-12 production compared to α-GalCer. Strikingly, this strong response was independent from the administration mode (soluble or loaded on BMDCs). Additionally all tested 6”-OH analogs induced a superior anti-tumor response compared to α-GalCer. PyrC-α-GalCer, the glycolipid which elicited the strongest cytokine response, was also most potent in preventing lung metastasis in a tumor model. Crystallographic analysis from the tri-molecular complex shows that this carbamate-analog forms increased and novel contacts with the TCR.

Because several diseases are characterized by an unbalanced cytokine response, skewing the iNKT Th1/Th2 response can be an interesting treatment option. Hence, understanding how glycolipid dependent iNKT cell activation can result in these contrasting cytokine profiles has been addressed by several groups and is important for the design of novel glycolipids with therapeutic properties. Different mechanisms both at the molecular and cellular level have been proposed. Recently, several reports have emphasized the stability of the CD1d-glycolipid complex to severely affect both the Th1 polarizing potency and the antigenicity of a glycolipid. This has been shown for structurally diverse glycolipids each displaying a different mechanism for the increased stability. First, alteration of the lipid chains by the introduction of aromatic or cyclopropane groups enhanced CD1d stability strengthened Th1 responses (6, 13, 48). Second, Tyznik et al. showed that introduction of cyclopropane groups in both acyl and sphingosine chain enhanced CD1d stability (6). Third, previous research from our own group showed that addition of extra linkers to the galactose could make additional contacts to CD1d, which resulted in increased CD1d stability and significantly more potent anti-tumor properties along with a Th1 polarized response. Fourth, although α-C-GalCer is a weaker antigen it was shown that its complex with CD1d had a prolonged half-life (5) probably because of its resistance towards enzymatic degradation by glycosidases. Our results reported here show that all novel carbamate analogs form complexes with the cell surface CD1d that are at least as stable as those with □-C-GalCer and NU-α-GalCer. This confirms the importance of the stability of the CD1d-glycolipid complex in the observed Th1 bias. Despite the apparent lateral binding of PyrC-α-GalCer above the A’ roof of CD1d, similar contacts are formed with CD1d when compared to the binding NU-α-GalCer, which binds in between the α1-α2 helix. Moreover, the tri-molecular structure with PyrC-α-GalCer shows novel additional contacts between

the TCR (residue Gln52) and the pyridine, which have previously not been seen in any other structure. Therefore we believe that our data provide a structural framework for the design of novel α-GalCer analogs that target Gln52 to increase TCR contacts. This enlargement of the TCR footprint may contribute to an enhanced stability of the tri-molecular complex and thus higher cytokine production.

The cytokine production of iNKT cells themselves cannot be polarized (49). However, polarization of the response depends mainly on the degree of activation of bystander cells, such as NK cells. It is believed that the IFN-γ which is initially produced by the iNKT cell itself, induces antigen presenting cells to produce IL-12 and IL-18 and subsequently drive NK cell dependent IFN-γ production (34, 50). Upregulation of co-stimulatory molecules is crucial for the onset of this IL-12 production (36, 41, 51) and plays an important role in the polarization of the iNKT cell response. Increased upregulation of co-stimulatory molecules might be linked to increased stability of the tri-molecular complex because a more stable immunological synapse might have more time for recruitment of these molecules. However, at present this hypothesis remains to be proven. The superior Th1 effect of □-C-GalCer has been attributed to superior induction of CD40 and CD40L ligation compared to α-GalCer (3). Our results indicate markedly increased IL-12 production along with an enhanced upregulation of CD40 and OX40L by PyrC-α-GalCer-pulsed-BMDC compared to NU-α-GalCer- and α-GalCer-pulsed-BMDCs, confirming that co-stimulation has an important role in expanding Th1 signalization. Two other co-stimulatory molecules, CD80 and CD86 were already almost maximally upregulated with α-GalCer. Therefore, no additional increase with 6”-OH altered glycolipids could be observed. This is in line with Fujii et al (2003), who found that CD80 and CD86 expression is less essential for adjuvant characteristics of glycolipids compared to CD40 (37). Th2 polarizing glycolipids are generally more hydrophilic and thus characterized by shorter lipid tails and/or insertion of unsaturated bounds into the lipid tails (2, 4, 52). These glycolipids are rather loaded onto CD1d at the cell surface and additionally these hydrophilic glycolipids are rapidly displaced from CD1d in the lysosome (4). In contrast, facilitated loading by lipid transfer proteins in the lysosome is essential for Th1 and mixed Th1/Th2 glycolipids. Additionally, cell surface loading of CD1d has been associated with presentation of the CD1d-glycolipid complex outside of lipid rafts. This is postulated to confer to a different immunological synapse and hence results, e.g. by exclusion of certain costimulatory markers and in less IFN-γ production by bystander NK cells (2). Although we did not specifically test the involvement of lipid rafts or lysosomal loading the fact that both strategies (loading onto BMDCs and soluble injection) resulted in a comparable Th1 polarization excludes an important role for differential loading of glycolipids. CD1d requires its cytoplasmic tail for recycling to the lysosome so antigen-presenting cells expressing the tail-deleted form of CD1d are not able to load lysosomal glycolipids. We previously

found that NU-α-GalCer and α-GalCer displayed similar results when presented by antigen presenting cells with the tail deleted form of CD1d indicating that 6''-derived glycolipids have a similar requirement for lysosomal loading as α-GalCer. Additional insertion of aromatic groups at the carbohydrate head moiety will probably not affect stability of the CD1d-glycolipid complex in the acid milieu of the lysosome because this is mainly due to lipid back bone alterations, which makes this unlikely to be an explanation for our results.

In conclusion, we show that structural optimization may afford analogues that combine increased Th1 potency (both in mice and men) with significantly stronger anti-cancer responses. Additionally PyrC-α-GalCer administration induces a 10-fold increase of IL-12 levels and is accompanied by increased upregulation of several costimulatory markers, which adds to its superior anti-tumor effect compared to NU-α-GalCer and α-GalCer. Crystallographic analysis revealed a previously unknown flexibility of the NKTCR footprint and therefore opens new avenues for the synthesis of novel Th1 polarizing glycolipids with therapeutical potential in the cancer research.

Acknowledgements

Tine Decruy, Julie Coudenys for ELISA, Kim Deswarte for FACS Sort, Masaru Taniguchi for Ja18-/- mice, Moriya Tsuji and the NIH Tetramer Core facility for providing α-C-GalCer, Stijn Lambrecht for help with statistical analysis.

Author contributions

S.A. performed and designed mouse experiments, K.V. performed human iNKT cell experiments, M.N. performed SPR and crystallographic experiments, N.P. and S.V.C. synthesized the glycolipids, S.A., M.N., D.M.Z. and D.E. designed experiments and analyzed the data; and S.A., M.N., D.M.Z. and D.E. wrote the manuscript.

References

1. Wu, L., and L. Van Kaer. 2011. Natural killer T cells in health and disease. *Front Biosci (Schol Ed)* 3:236-251.
2. Fujii, S., K. Shimizu, H. Hemmi, M. Fukui, A. J. Bonito, G. Chen, R. W. Franck, M. Tsuji, and R. M. Steinman. 2006. Glycolipid alpha-C-galactosylceramide is a distinct inducer of dendritic cell function during innate and adaptive immune responses of mice. *Proc Natl Acad Sci U S A* 103:11252-11257.
3. Im, J. S., P. Arora, G. Bricard, A. Molano, M. M. Venkataswamy, I. Baine, E. S. Jerud, M. F. Goldberg, A. Baena, K. O. Yu, R. M. Ndonye, A. R. Howell, W. Yuan, P. Cresswell, Y. T. Chang, P. A. Illarionov, G. S. Besra, and S. A. Porcelli. 2009. Kinetics and cellular site of glycolipid loading control the outcome of natural killer T cell activation. *Immunity* 30:888-898.
4. Bai, L., Y. Sagiv, Y. Liu, S. Freigang, K. O. Yu, L. Teyton, S. A. Porcelli, P. B. Savage, and A. Bendelac. 2009. Lysosomal recycling terminates CD1d-mediated presentation of short and polyunsaturated variants of the NKT cell lipid antigen alphaGalCer. *Proc Natl Acad Sci U S A* 106:10254-10259.
5. Sullivan, B. A., N. A. Nagarajan, G. Wingender, J. Wang, I. Scott, M. Tsuji, R. W. Franck, S. A. Porcelli, D. M. Zajonc, and M. Kronenberg. 2010. Mechanisms for glycolipid antigen-driven cytokine polarization by Valpha14i NKT cells. *J Immunol* 184:141-153.
6. Tyznik, A. J., E. Farber, E. Girardi, A. Birkholz, Y. Li, S. Chitale, R. So, P. Arora, A. Khurana, J. Wang, S. A. Porcelli, D. M. Zajonc, M. Kronenberg, and A. R. Howell. 2011. Glycolipids that Elicit IFN-gamma-Biased Responses from Natural Killer T Cells. *Chem Biol* 18:1620-1630.
7. Aspeslagh, S., Y. Li, E. D. Yu, N. Pauwels, M. Trappeniers, E. Girardi, T. Decruy, K. Van Beneden, K. Venken, M. Drennan, L. Leybaert, J. Wang, R. W. Franck, S. Van Calenbergh, D. M. Zajonc, and D. Elewaut. 2011. Galactose-modified iNKT cell agonists stabilized by an induced fit of CD1d prevent tumour metastasis. *EMBO J* 30:2294-2305.
8. Venkataswamy, M. M., and S. A. Porcelli. 2010. Lipid and glycolipid antigens of CD1d-restricted natural killer T cells. *Semin Immunol* 22:68-78.
9. Joyce, S., E. Girardi, and D. M. Zajonc. 2011. NKT cell ligand recognition logic: molecular basis for a synaptic duet and transmission of inflammatory effectors. *J Immunol* 187:1081-1089.
10. Scott-Browne, J. P., J. L. Matsuda, T. Mallevaey, J. White, N. A. Borg, J. McCluskey, J. Rossjohn, J. Kappler, P. Marrack, and L. Gapin. 2007. Germline-encoded recognition of diverse glycolipids by natural killer T cells. *Nat Immunol* 8:1105-1113.
11. Fujio, M., D. Wu, R. Garcia-Navarro, D. D. Ho, M. Tsuji, and C. H. Wong. 2006. Structure-based discovery of glycolipids for CD1d-mediated NKT cell activation: tuning the adjuvant versus immunosuppression activity. *J Am Chem Soc* 128:9022-9023.
12. Liang, P. H., M. Imamura, X. Li, D. Wu, M. Fujio, R. T. Guy, B. C. Wu, M. Tsuji, and C. H. Wong. 2008. Quantitative microarray analysis of intact glycolipid-CD1d interaction and correlation with cell-based cytokine production. *J Am Chem Soc* 130:12348-12354.
13. Wu, T. N., K. H. Lin, Y. J. Chang, J. R. Huang, J. Y. Cheng, A. L. Yu, and C. H. Wong. 2011. Avidity of CD1d-ligand-receptor ternary complex contributes to T-helper 1 (Th1) polarization and anticancer efficacy. *Proc Natl Acad Sci U S A* 108:17275-17280.
14. Wun, K. S., G. Cameron, O. Patel, S. S. Pang, D. G. Pellicci, L. C. Sullivan, S. Keshipeddy, M. H. Young, A. P. Uldrich, M. S. Thakur, S. K. Richardson, A. R. Howell, P. A. Illarionov, A. G. Brooks, G. S. Besra, J. McCluskey, L. Gapin, S. A. Porcelli, D. I. Godfrey, and J. Rossjohn. 2011. A molecular basis for the exquisite CD1d-restricted antigen specificity and functional responses of natural killer T cells. *Immunity* 34:327-339.

15. Girardi, E., E. D. Yu, Y. Li, N. Tarumoto, B. Pei, J. Wang, P. Illarionov, Y. Kinjo, M. Kronenberg, and D. M. Zajonc. 2011. Unique interplay between sugar and lipid in determining the antigenic potency of bacterial antigens for NKT cells. *PLoS Biol* 9:e1001189.
16. Li, Y., E. Girardi, J. Wang, E. D. Yu, G. F. Painter, M. Kronenberg, and D. M. Zajonc. 2010. The V{alpha}14 invariant natural killer T cell TCR forces microbial glycolipids and CD1d into a conserved binding mode. *J Exp Med*.
17. Yu, E. D., E. Girardi, J. Wang, and D. M. Zajonc. 2011. Cutting Edge: Structural basis for the recognition of beta-linked glycolipid antigens by invariant NKT cells. *J Immunol* 187:2079-2083.
18. Pellicci, D. G., A. J. Clarke, O. Patel, T. Mallevaey, T. Beddoe, J. Le Nours, A. P. Uldrich, J. McCluskey, G. S. Besra, S. A. Porcelli, L. Gapin, D. I. Godfrey, and J. Rossjohn. 2011. Recognition of beta-linked self glycolipids mediated by natural killer T cell antigen receptors. *Nat Immunol* 12:827-833.
19. Trappeniers, M., K. Van Beneden, T. Decruy, U. Hillaert, B. Linclau, D. Elewaut, and S. Van Calenbergh. 2008. 6'-derivatised alpha-GalCer analogues capable of inducing strong CD1d-mediated Th1-biased NKT cell responses in mice. *J Am Chem Soc* 130:16468-16469.
20. Burdin, N., L. Brossay, Y. Koezuka, S. T. Smiley, M. J. Grusby, M. Gui, M. Taniguchi, K. Hayakawa, and M. Kronenberg. 1998. Selective ability of mouse CD1 to present glycolipids: alpha-galactosylceramide specifically stimulates V alpha 14+ NK T lymphocytes. *J Immunol* 161:3271-3281.
21. Lutz, M. B., N. Kukutsch, A. L. Ogilvie, S. Rossner, F. Koch, N. Romani, and G. Schuler. 1999. An advanced culture method for generating large quantities of highly pure dendritic cells from mouse bone marrow. *J Immunol Methods* 223:77-92.
22. Cui, J., T. Shin, T. Kawano, H. Sato, E. Kondo, I. Toura, Y. Kaneko, H. Koseki, M. Kanno, and M. Taniguchi. 1997. Requirement for Valpha14 NKT cells in IL-12-mediated rejection of tumors. *Science* 278:1623-1626.
23. Franki, A. S., K. Van Beneden, P. Dewint, K. J. Hammond, S. Lambrecht, G. Leclercq, M. Kronenberg, D. Deforce, and D. Elewaut. 2006. A unique lymphotoxin {alpha}beta-dependent pathway regulates thymic emigration of V{alpha}14 invariant natural killer T cells. *Proc Natl Acad Sci U S A* 103:9160-9165.
24. Wang, J., Y. Li, Y. Kinjo, T. T. Mac, D. Gibson, G. F. Painter, M. Kronenberg, and D. M. Zajonc. 2010. Lipid binding orientation within CD1d affects recognition of Borrelia burgorferi antigens by NKT cells. *Proc Natl Acad Sci U S A* 107:1535-1540.
25. Otwinowski, Z. M. W. 1997. Processing of X-ray Diffraction Data Collected in Oscillation Mode. *Methods in Enzymology* 276:307-326.
26. Leslie, A. G., and H. R. Powell. 2007. Evolving Methods for Macromolecular Crystallography. 245:41-51.
27. Vagin, A. A., and A. Teplyakov. 1997. MOLREP: an automated program for molecular replacement. *J. Appl. Cryst* 30:1022-1025.
28. Winn, M. D., C. C. Ballard, K. D. Cowtan, E. J. Dodson, P. Emsley, P. R. Evans, R. M. Keegan, E. B. Krissinel, A. G. Leslie, A. McCoy, S. J. McNicholas, G. N. Murshudov, N. S. Pannu, E. A. Potterton, H. R. Powell, R. J. Read, A. Vagin, and K. S. Wilson. 2011. Overview of the CCP4 suite and current developments. *Acta Crystallogr D Biol Crystallogr* 67:235-242.
29. Schuttelkopf, A. W., and D. M. van Aalten. 2004. PRODRG: a tool for high-throughput crystallography of protein-ligand complexes. *Acta Crystallogr D Biol Crystallogr* 60:1355-1363.
30. Emsley, P., and K. Cowtan. 2004. Coot: model-building tools for molecular graphics. *Acta Crystallogr D Biol Crystallogr* 60:2126-2132.

31. Vagin, A. A., R. A. Steiner, A. A. Lebedev, L. Potterton, S. McNicholas, F. Long, and G. N. Murshudov. 2004. REFMAC5 dictionary: organization of prior chemical knowledge and guidelines for its use. *Acta Crystallogr D Biol Crystallogr* 60:2184-2195.
32. Chen, V. B., W. B. Arendall, 3rd, J. J. Headd, D. A. Keedy, R. M. Immormino, G. J. Kapral, L. W. Murray, J. S. Richardson, and D. C. Richardson. 2010. MolProbity: all-atom structure validation for macromolecular crystallography. *Acta Crystallogr D Biol Crystallogr* 66:12-21.
33. Pauwels, N., S. Aspeslagh, G. Vanhoenacker, K. Sandra, E. D. Yu, D. M. Zajonc, D. Elewaut, B. Linclau, and S. Van Calenbergh. 2011. Divergent synthetic approach to 6"-modified alpha-GalCer analogues. *Org Biomol Chem* 9:8413-8421.
34. Smyth, M. J., N. Y. Crowe, D. G. Pellicci, K. Kyparissoudis, J. M. Kelly, K. Takeda, H. Yagita, and D. I. Godfrey. 2002. Sequential production of interferon-gamma by NK1.1(+) T cells and natural killer cells is essential for the antimetastatic effect of alpha-galactosylceramide. *Blood* 99:1259-1266.
35. Wesley, J. D., S. H. Robbins, S. Sidobre, M. Kronenberg, S. Terrizzi, and L. Brossay. 2005. Cutting edge: IFN-gamma signaling to macrophages is required for optimal Valpha14i NK T/NK cell cross-talk. *J Immunol* 174:3864-3868.
36. Vincent, M. S., D. S. Leslie, J. E. Gumperz, X. Xiong, E. P. Grant, and M. B. Brenner. 2002. CD1-dependent dendritic cell instruction. *Nat Immunol* 3:1163-1168.
37. Fujii, S., K. Shimizu, C. Smith, L. Bonifaz, and R. M. Steinman. 2003. Activation of natural killer T cells by alpha-galactosylceramide rapidly induces the full maturation of dendritic cells in vivo and thereby acts as an adjuvant for combined CD4 and CD8 T cell immunity to a coadministered protein. *J Exp Med* 198:267-279.
38. Zaini, J., S. Andarini, M. Tahara, Y. Saijo, N. Ishii, K. Kawakami, M. Taniguchi, K. Sugamura, T. Nukiwa, and T. Kikuchi. 2007. OX40 ligand expressed by DCs costimulates NKT and CD4+ Th cell antitumor immunity in mice. *J Clin Invest* 117:3330-3338.
39. Zietara, N., M. Lyszkiewicz, A. Krueger, and S. Weiss. 2011. ICOS-dependent stimulation of NKT cells by marginal zone B cells. *Eur J Immunol* 41:3125-3134.
40. Akbari, O., P. Stock, E. H. Meyer, G. J. Freeman, A. H. Sharpe, D. T. Umetsu, and R. H. DeKruyff. 2008. ICOS/ICOSL interaction is required for CD4+ invariant NKT cell function and homeostatic survival. *J Immunol* 180:5448-5456.
41. Hayakawa, Y., K. Takeda, H. Yagita, L. Van Kaer, I. Saiki, and K. Okumura. 2001. Differential regulation of Th1 and Th2 functions of NKT cells by CD28 and CD40 costimulatory pathways. *J Immunol* 166:6012-6018.
42. Bezbradica, J. S., A. K. Stanic, N. Matsuki, H. Bour-Jordan, J. A. Bluestone, J. W. Thomas, D. Unutmaz, L. Van Kaer, and S. Joyce. 2005. Distinct Roles of Dendritic Cells and B Cells in Va14Ja18 Natural T Cell Activation In Vivo. *J Immunol* 174:4696-4705.
43. Bai, L., M. G. Constantinides, S. Y. Thomas, R. Reboulet, F. Meng, F. Koentgen, L. Teyton, P. B. Savage, and A. Bendelac. 2012. Distinct APCs explain the cytokine bias of alpha-galactosylceramide variants in vivo. *J Immunol* 188:3053-3061.
44. Sidobre, S., O. V. Naidenko, B. C. Sim, N. R. Gascoigne, K. C. Garcia, and M. Kronenberg. 2002. The V alpha 14 NKT cell TCR exhibits high-affinity binding to a glycolipid/CD1d complex. *J Immunol* 169:1340-1348.
45. Granucci, F., C. Vizzardelli, N. Pavelka, S. Feau, M. Persico, E. Virzi, M. Rescigno, G. Moro, and P. Ricciardi-Castagnoli. 2001. Inducible IL-2 production by dendritic cells revealed by global gene expression analysis. *Nat Immunol* 2:882-888.
46. Wilson, M. T., C. Johansson, D. Olivares-Villagomez, A. K. Singh, A. K. Stanic, C. R. Wang, S. Joyce, M. J. Wick, and L. Van Kaer. 2003. The response of natural killer T cells to glycolipid antigens is characterized by surface receptor down-modulation and expansion. *Proc Natl Acad Sci U S A* 100:10913-10918.

47. Li, X., M. Fujio, M. Imamura, D. Wu, S. Vasan, C. H. Wong, D. D. Ho, and M. Tsuji. 2011. Design of a potent CD1d-binding NKT cell ligand as a vaccine adjuvant. *Proc Natl Acad Sci U S A* 107:13010-13015.
48. Schiefner, A., M. Fujio, D. Wu, C. H. Wong, and I. A. Wilson. 2009. Structural evaluation of potent NKT cell agonists: implications for design of novel stimulatory ligands. *J Mol Biol* 394:71-82.
49. Matsuda, J. L., L. Gapin, J. L. Baron, S. Sidobre, D. B. Stetson, M. Mohrs, R. M. Locksley, and M. Kronenberg. 2003. Mouse V alpha 14i natural killer T cells are resistant to cytokine polarization in vivo. *Proc Natl Acad Sci U S A* 100:8395-8400.
50. Wesley, J. D., M. S. Tessmer, D. Chaukos, and L. Brossay. 2008. NK cell-like behavior of Valpha14i NK T cells during MCMV infection. *PLoS Pathog* 4:e1000106.
51. van den Heuvel, M. J., N. Garg, L. Van Kaer, and S. M. Haeryfar. 2011. NKT cell costimulation: experimental progress and therapeutic promise. *Trends Mol Med* 17:65-77.
52. Yu, K. O., J. S. Im, A. Molano, Y. Dutronc, P. A. Illarionov, C. Forestier, N. Fujiwara, I. Arias, S. Miyake, T. Yamamura, Y. T. Chang, G. S. Besra, and S. A. Porcelli. 2005. Modulation of CD1d-restricted NKT cell responses by using N-acyl variants of alpha-galactosylceramides. *Proc Natl Acad Sci U S A* 102:3383-3388.

Figure Legend

Figure 1

Th1–Th2 profile of novel glycolipids: serum cytokine levels at 16 hours after injection of 5 µg glycolipid (i.p.). Graphs indicate the mean with s.e.m. of at least sixteen mice. Data are of pooled of two independent experiments. (a) IFN-γ levels of α-GalCer and NU-α-GalCer are significantly lower (at least $p<0.05$ as indicated by * for α-GalCer for and # for NU-α-GalCer) compared with 4ClPhC-, NC- and PyrC-α-GalCer (Kruskal–Wallis test, two tailed Mann-Whitney U-test), the p-value of NC-α-GalCer compared to α-GalCer is equal to 0.0552. (b) IL-12 levels of α-GalCer are significantly lower compared with 4ClPhC-, NC- and PyrC-α-GalCer (at least $p<0.05$ as indicated by * for α-GalCer for and # for NU-α-GalCer), additionally PyrC-α-GalCer induces significantly higher IL-12 levels ($p<0.001$). (Kruskal–Wallis test, two- tailed Mann–Whitney U-test).

Figure 2

Th1–Th2 profile of novel glycolipids loaded on BMDCs (20h, 100 ng/mL): serum cytokine levels at different time points after injection of glycolipid pulsed BMDCs. Graphs indicate the mean with s.e.m. of at least sixteen mice. Data are of pooled of two independent experiments. (a) After injection of 600 000 glycolipid-pulsed BMDCs IFN-γ levels of 4ClPhC- and PyrC-α-GalCer are both at 16 and 24 hours significantly higher compared to NU-α-GalCer. NU-α-GalCer also induces IFN-γ levels that are significantly higher compared to α-GalCer both at 16 and 24 hours after injection. (at least $p<0.05$ as indicated by * for α-GalCer for and # for NU-α-GalCer) (Kruskal-Wallis test and two-tailed Mann-Whitney U test). (b) After injection of 600 000 glycolipid-pulsed BMDCs, IL-12 levels of PyrC-α-GalCer are both at 16 and 24 hours significantly higher compared to NU-α-GalCer. NU-α-GalCer and 4ClPhC also induce IFN-□ levels that are significantly higher compared to α-GalCer at 16 hours after injection. ($p<0.001$ as indicated by * for α-GalCer for and # for NU-α-GalCer) (Kruskal-Wallis test and two-tailed Mann-Whitney U test). (c) + (d) Both IFN-γ and IL-12 levels are significantly higher 16 hours after injection of only 10 000 PyrC-pulsed BMDCs compared to NU-α-GalCer and α-GalCer. (at least $p<0.01$ as indicated by * for α-GalCer for and # for NU-α-GalCer) (Kruskal-Wallis test and two-tailed Mann-Whitney U test)

Figure 3

Cytokine levels in supernatant of co-culture of human iNKT cells and glycolipid-loaded irradiated PBMC. Results shown are pooled data from two independent experiments using cells from two different donors. (a) Analysis of Th2 cytokines shows less production of IL-13 and IL-4

for PyrC-α-GalCer compared to α-GalCer stimulated iNKT cells (Mann-Whitney U test p=0.02 for IFN-γ and ns for IL-4). (b) In contrast, IFN-γ and IL-12 production are slightly elevated with PyrC-α-GalCer compared to α-GalCer (Mann-Whitney U test p=0.03 for IFN-γ and p=0.05 for IL-12).

Figure 4

***In vitro* stimulation of an iNKT cell line with 6'-OH altered glycolipids bound to bone marrow-derived dendritic cells (BMDCs).** BMDCs were grown with GM-CSF for 10 days and subsequently loaded with a glycolipid (100 ng/ml) for 20 h. (a) Co-culture with an iNKT cell line (2C12) was set up for 16 hours and IL-2 production was measured by ELISA. 4ClPhC-, NC-, PyrC-α-GalCer, and NU-α-GalCer significantly differ from α-GalCer ($p<0.01$) (two- tailed Mann–Whitney U-test). Data are shown as mean with s.e.m. (n=6). One representative of seven independent experiments. (b) TCR□ expression by the iNKT cell line (2C12) 24 hours after coculture with glycolipid-pulsed CD45.1 BMDCs. iNKT cells were selected as CD45.2 positive, CD45.1 negative and 7AAD negative. All 6"-OH altered glycolipids including α-C-GalCer show clear TCRb downregulation. One representative experiment of two independent experiments. (c) Intracellular IL-2 production by 2C12 cells, 4 hours after coculture. One representative of two independent experiments.

Figure 5

Analysis of stability of the glycolipid-CD1d complex (a) Bone marrow dendritic cells were first loaded during 20 hours with 100 ng/mL glycolipid. Hereafter the glycolipid was washed away, cells were left in appropriate medium for several time intervals (ranging form 4 h to 48 h, see X-axis). Medium with glycolipid that might have come off CD1d was washed away and coculture with 2C12 cells (iNKT cell hybridoma). IL-2 production in the medium was used as a surrogate marker for glycolipid-loaded CD1d complexes. (b) Data from (a) were normalized to the 4 hour time point. Represents stability of each glycolipid towards CD1d. Data are shown as mean with s.e.m. (n = 6). One representative of two independent experiments.

Figure 6

Crystal structure of the mCD1d-4ClPhC-α-GalCer-mTCR and mCD1d-PyrC-α-GalCer-mTCR ternary complexes. (a) Overview of the representative ternary complex containing PyrC-α-GalCer. PyrC-α-GalCer is shown in orange, mCD1d heavy chain in grey and β2m in purple. TCR α chain is shown in cyan and TCR β chain is shown in orange. (b) Final $2F_o$-F_c electron density map is shown as blue mesh, contoured at 1.0 σ level for the glycolipid PyrC-α-GalCer (upper panel) and for 4ClPhC-α-GalCer (lower panel, in yellow). Note that α2-helix is removed for clarity. (c) TCR glycolipid contacts illustrate the additional TCR contact between the Q52 and the nitrogen of the

aromatic group of PyrC-α-GalCer (top panel), while both ligands lack the H-bond between 4'-OH of galactose with N30 of TCR. Hydrogen bonds are indicated as dotted lines. While the 4ClPhC-α-GalCer assumes a more intimate position with CD1d (lower panel), PyrC-α-GalCer is tilted upward to interact more closely with the TCR (upper panel). (d) H-bond interactions between mCD1d and both glycolipids is conserved.

Figure 7

Binding comparison of Th1-skewing NKT cell antigen. Superimposing the structures of mCD1d-α-GalCer-mTCR (PDB code 3HE6, purple), mCD1d-NU-GalCer-mTCR (PDB code 3QUZ, green), mCD1d-PyrC-α-GalCer-mTCR (PDB code 4IRS, orange) and mCD1d-4ClPhC-α-GalCer-mTCR (PDB code 4IRJ, yellow) complexes indicate differences in accommodating the 6'-OH substitutions of each glycolipid. Carbamate linked functional groups are situated laterally above the CD1d binding group (4ClPhC-α-GalCer) or tilted toward the TCR (PyrC-α-GalCer), while NU-α-GalCer is inserted into the CD1d binding group.

Figure 8

Tumor suppression by iNKT cell stimulation in a B16 melanoma lung metastasis model. (a) When 10 000 BMDCs loaded with glycolipid were injected, all 6'-OH altered glycolipids are able to reduce the quantity of lung nodules significantly more than α-GalCer. Additionally PyrC-α-GalCer is able to reduce the amount of noduli even significantly better. Each dot represents an individual mouse with at least 8 mice/group. Data are representative of two independent experiments. Error bars express mean and Kruskal-Wallis test and one-sided Student t-test was used for statistical analysis. (b) Pictures of lungs that were used for analysis in (a). Each lung is representative for the specific glycolipid as the lung with the amount of lung noduli that is the closest to the mean (number in the left corner) are represented here.

Table I

TCR binding kinetics

Table II

Buried surface areas between TCR-CD1d and glycolipid (in $Å^2$)

Footnotes

---

[i] S.A. and K.V. are recipients of fellowships supported by FWO Flanders. M.N is supported by the Slovak American Foundation. D.E. and S.V.C received support of the Belgian Stichting tegen Kanker, the FWO Flanders and the research council of Ghent University. D.M.Z is supported by NIH grant RO1 AI074952. Portions of this research were carried out at the Stanford Synchrotron Radiation Lightsource, a Directorate of SLAC National Accelerator Laboratory and an Office of Science User Facility operated for the U.S. Department of Energy Office of Science by Stanford University. The SSRL Structural Molecular Biology Program is supported by the DOE Office of Biological and Environmental Research, and by the National Institutes of Health, National Institute of General Medical Sciences (including P41GM103393) and the National Center for Research Resources (P41RR001209).

[ii] Structure factors and coordinates have been deposited in Protein Data Bank (www.rcsb.org) under accession code 4IRJ (4ClPhC-alpha-GalCer), 4IRS (PyrC-alpha-GalCer).

Abbreviations used in this paper: BMDC: bone marrow dendritic cell, NKT cell: natural killer T cell, NKTCR: NKT cell T cell receptor; α-GalCer : alpha galactosyl ceramide, 4ClPhC-α-GalCer: α-GalCer-6”-(4-chlorophenyl)carbamate, NC-α-GalCer: α-GalCer-6”-(1-naphthyl)carbamate, NU-α-GalCer: α-GalCer-6”-(1-naphthyl)urea, PyrC-α-GalCer: α-GalCer-6”-(pyridin-4-yl)carbamate

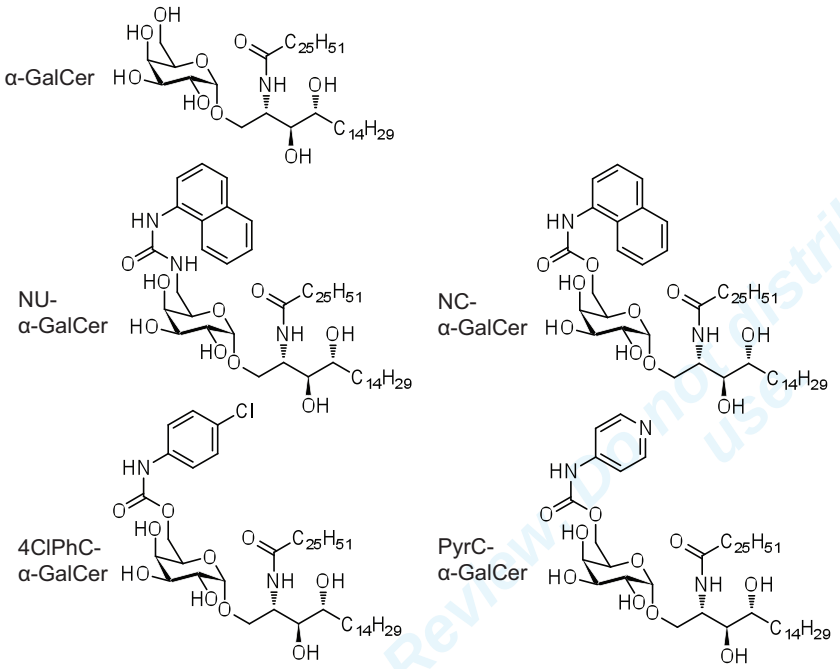

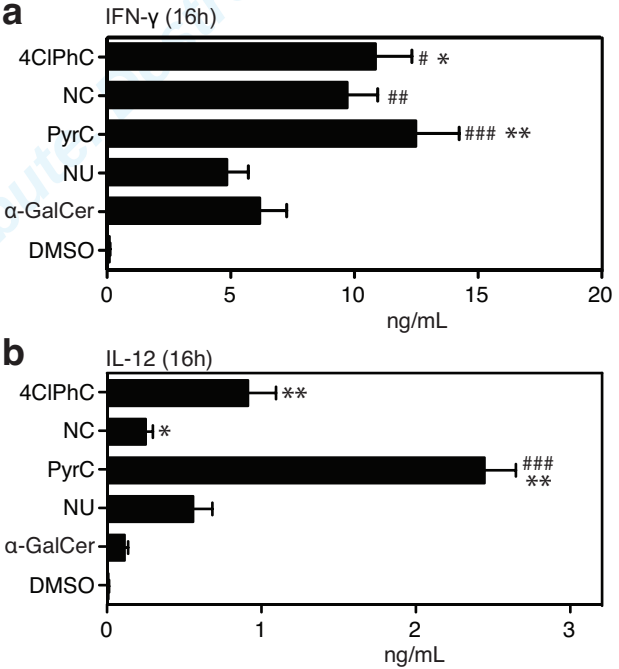

Figure 1

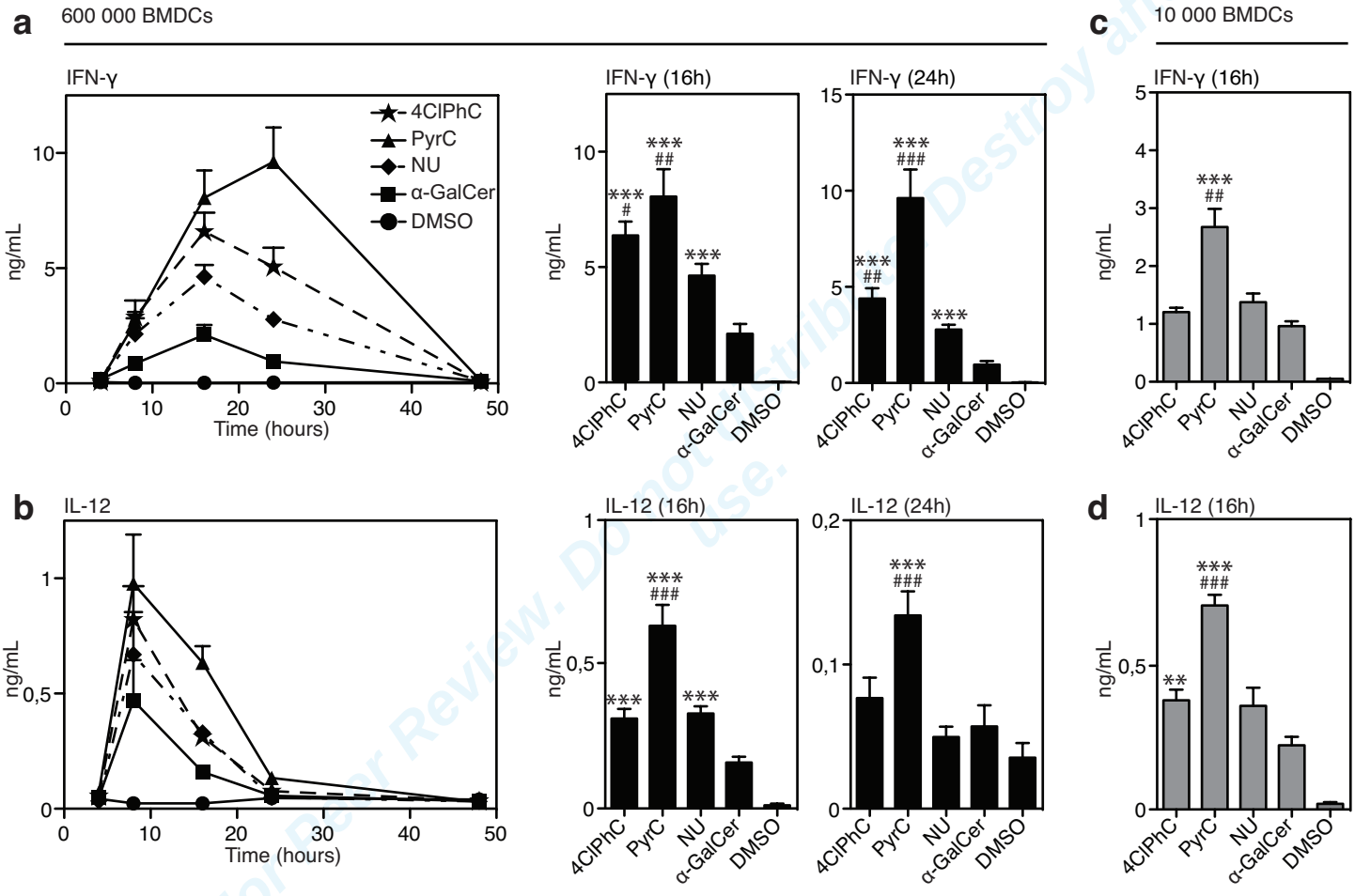

Figure 2

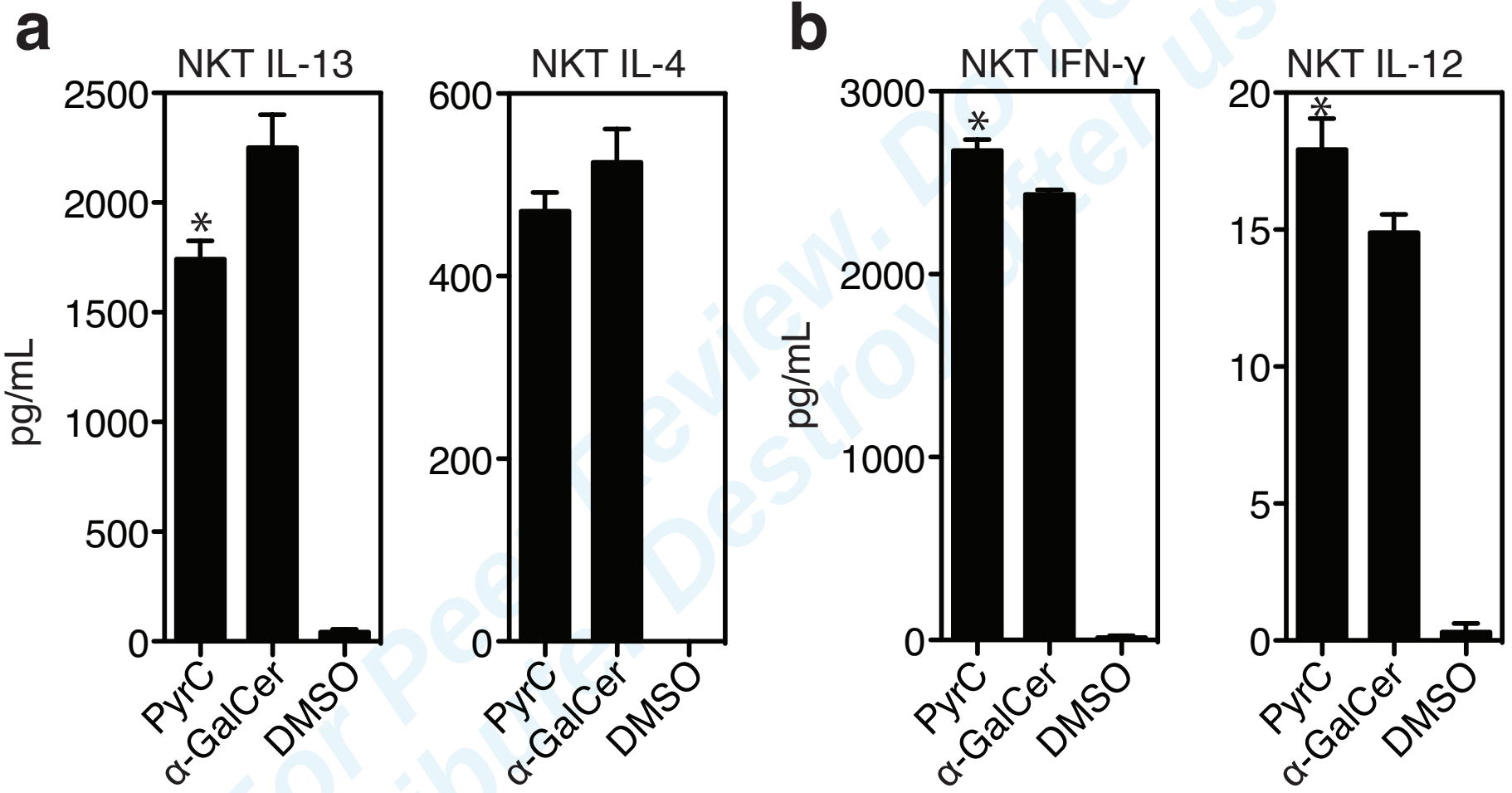

Figure 3

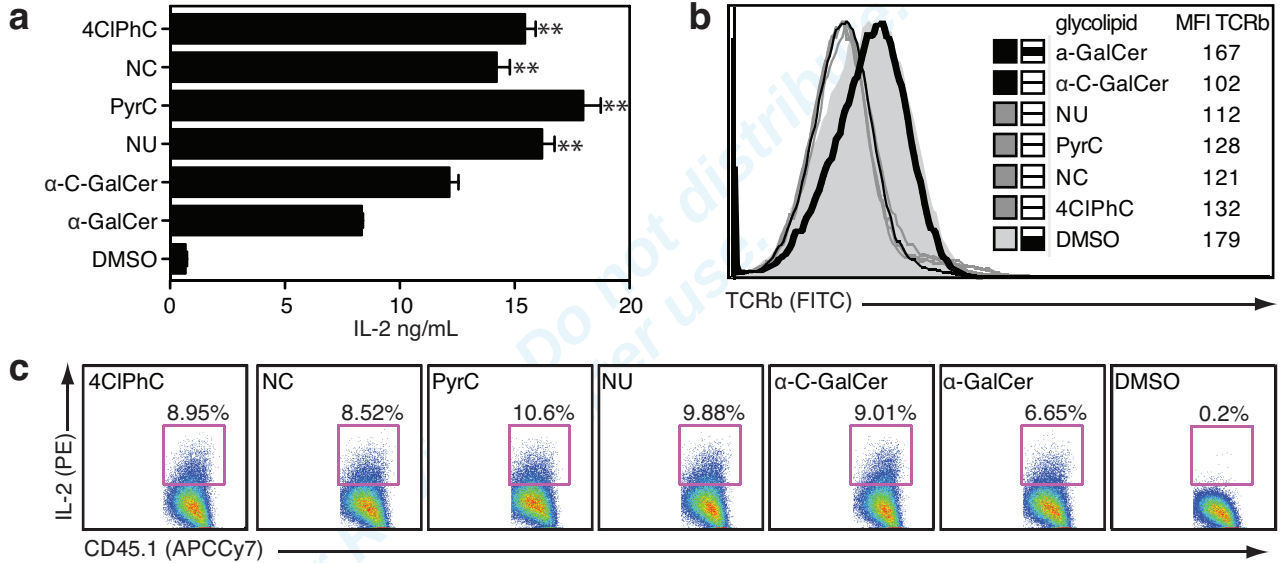
a
4ClPhC
NC
PyrC
NU
α-C-GalCer
α-GalCer
DMSO
**
**
**
**
0
5
10
15
20
IL-2 ng/mL
b
glycolipid
MFI TCRb
a-GalCer 167
α-C-GalCer 102
NU 112
PyrC 128
NC 121
4ClPhC 132
DMSO 179
TCRb (FITC)
c
4ClPhC
8.95%
NC
8.52%
PyrC
10.6%
NU
9.88%
α-C-GalCer
9.01%
α-GalCer
6.65%
DMSO
0.2%
IL-2 (PE)
CD45.1 (APCCy7)

Figure 4

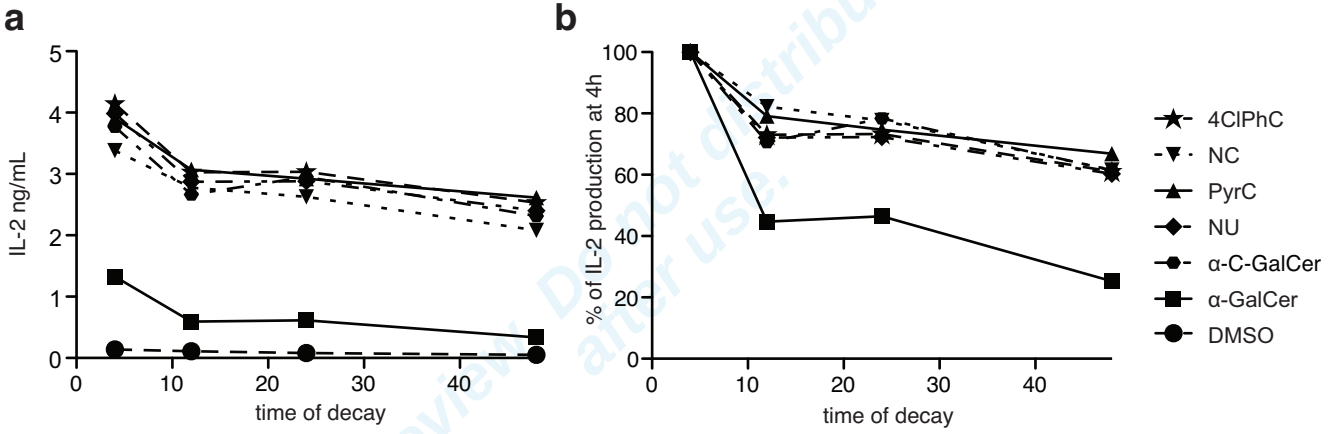
a
IL-2 ng/mL
time of decay
b
% of IL-2 production at 4h
time of decay
4ClPhC
NC
PyrC
NU
α-C-GalCer
α-GalCer
DMSO

Figure 5

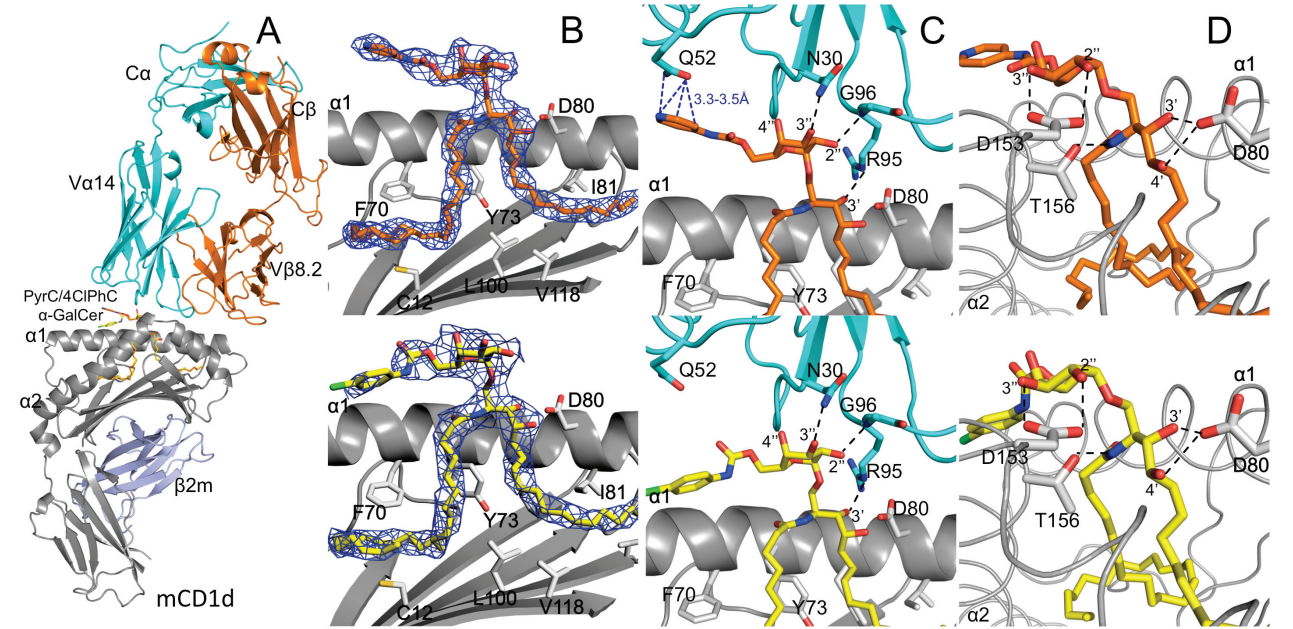
A
Cα
Cβ
Vα14
Vβ8.2
PyrC/4ClPhC
α-GalCer
α1
α2
β2m
mCD1d
B
α1
D80
I81
F70
Y73
C12
L100
V118
C
Q52
N30
3.3-3.5Å
G96
R95
D
D153
T156
α2

Figure 6

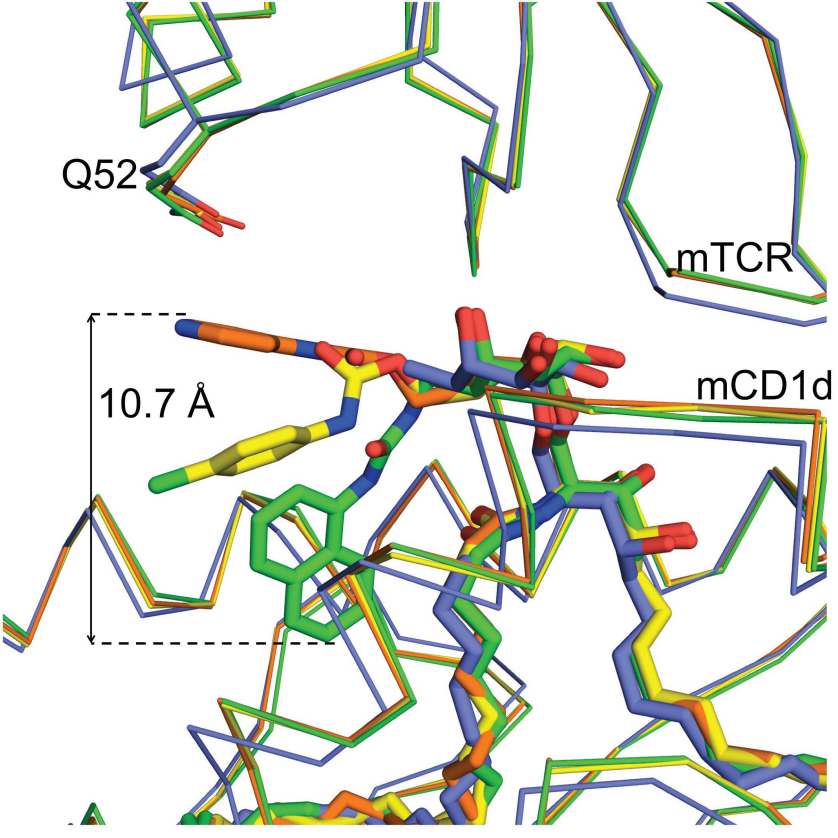

Figure 7

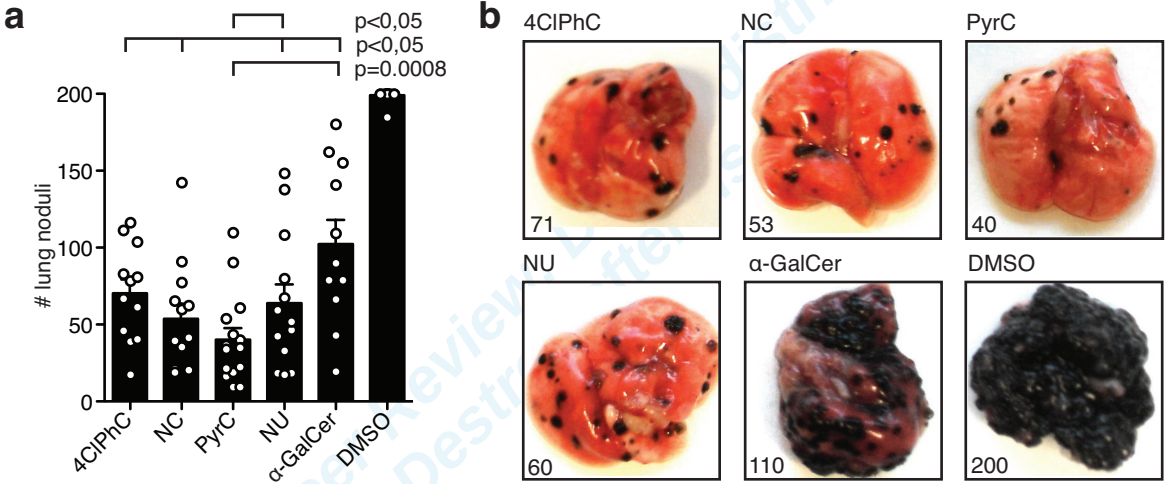
a
p<0,05
p<0,05
p=0.0008
200
150
100
50
0
lung noduli
4ClPhC
NC
PyrC
NU
α-GalCer
DMSO
b
4ClPhC
NC
PyrC
71
53
40
NU
α-GalCer
DMSO
60
110
200

Figure 8

Table 1. TCR binding kinetics

glycolipid	**K_D [nM]**	**k_{on} [$M^{-1}s^{-1}$]**	**k_{off} [s^{-1}]**	
α-GalCer	26.45±4.6	$5.06\pm0.66 10^{4}$	$1.34\pm0.09 10^{-3}$	
4ClPhC-α-GalCer	49.3±0.3	$5.27\pm1.47 10^{4}$	$2.62\pm0.72 10^{-3}$	
NC-α-GalCer	37.1±14	$3.83\pm0.53 10^{4}$	$1.5\pm0.074 10^{-3}$	
PyrC-α-GalCer	25.0±3	$6.61\pm1.21 10^{4}$	$1.61\pm0.01 10^{-3}$	

Table 2. Buried surface areas between TCR-CD1d and glycolipid (in Å^3)

	CD1d-ligand-TCR complex			
Contact surfaces	α-GalCer[1]	NU-α-GalCer	4ClPhC-α-GalCer	PyrC- α-GalCer
CD1d-ligand	1,027	1,146	1,124	1,045
TCRα-ligand	137.1	146.2	155.7	199.2
TCRα-CD1d	433.4	427.9	436.3	434.9
TCRβ-CD1d[1]	*192.6*	324.0	298.9	319.3
TCRαβ-CD1d[1]	*626*	751.9	735.2	754.2

[1]CDR3β sequence of the TCR found in the α-GalCer complex is different from CDR3β sequence found in all other structures and lacks contacts with CD1d. Therefore, contact surfaces TCRβ-CD1d and TCRαβ-CD1d are smaller.